

# High-Performance Micro Heat-Pipe

by Koji Yamamoto \*, Kenji Nakamizo \*,  
Hideaki Kameoka \*2 and Ken'ichi Namba \*3

**ABSTRACT** With greater electronic equipment speeds and higher performance, more heat is generated posing acute problems of heat dissipation. Accordingly, Furukawa Electric has been marketing heat sinks that incorporate micro heat-pipes since 1995. Whereas a number of products with different configurations and components have been developed over the years responding to ever increasing heat, the authors have recently improved thermal performance of micro heat-pipes per se in order to cope with further increases in heat generation expected in future.

## 1. INTRODUCTION

Recent developments of electronic equipment in terms of their speeds and performance are truly remarkable, posing at the same time the problem of increased heat generation that has to be dissipated. When in particular the equipment is required to be compact in size, as is the case with notebook PCs, heat dissipation technology is one of the key issues since this involves the stability and throughput performance of such equipment. Against this technological background, Furukawa Electric has been marketing heat sinks that incorporate micro heat-pipes

(hereafter denoted as  $\mu$ HP) since 1995.  $\mu$ HP generally refers to small-sized heat-pipes with a diameter of 3 to 6 mm, which can be utilized to realize compact heat sinks of high heat dissipation efficiency by incorporating such components as metal plate, heat radiation fin, fan, etc. Thus as shown in Figure 1, new products with different configurations and components have been developed as the heat generated by MPUs continued to increase. In this work, the authors have improved thermal performance of  $\mu$ HPs per se in order to cope with further increases in heat generation expected in future.

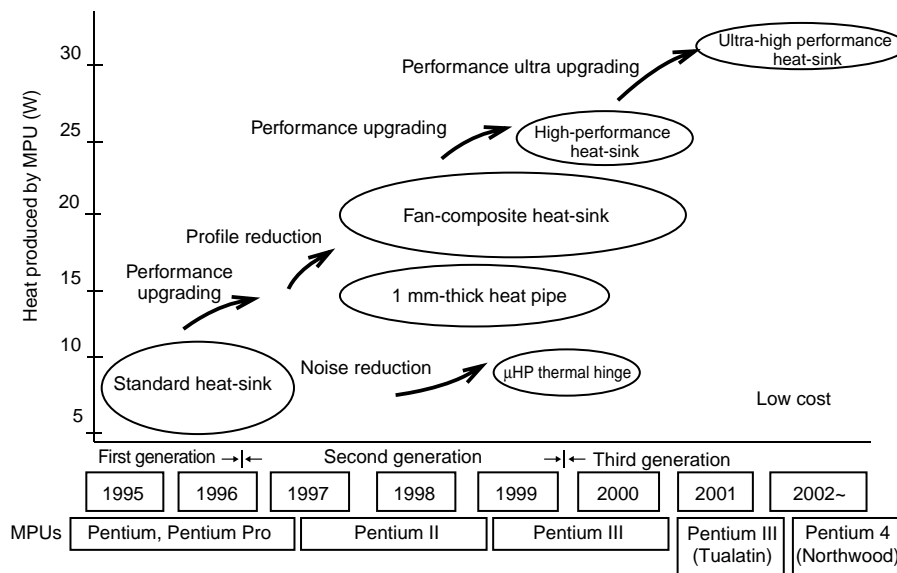


Figure 1 Changes in the development of  $\mu$ HP-based heat sink.

\* First Development Dept., Metal Research Center  
 \*2 Thermal Products Dept., Electronic Components Div.  
 \*3 Parts and Mounting Technology Development Dept., Ecology and Energy Lab.

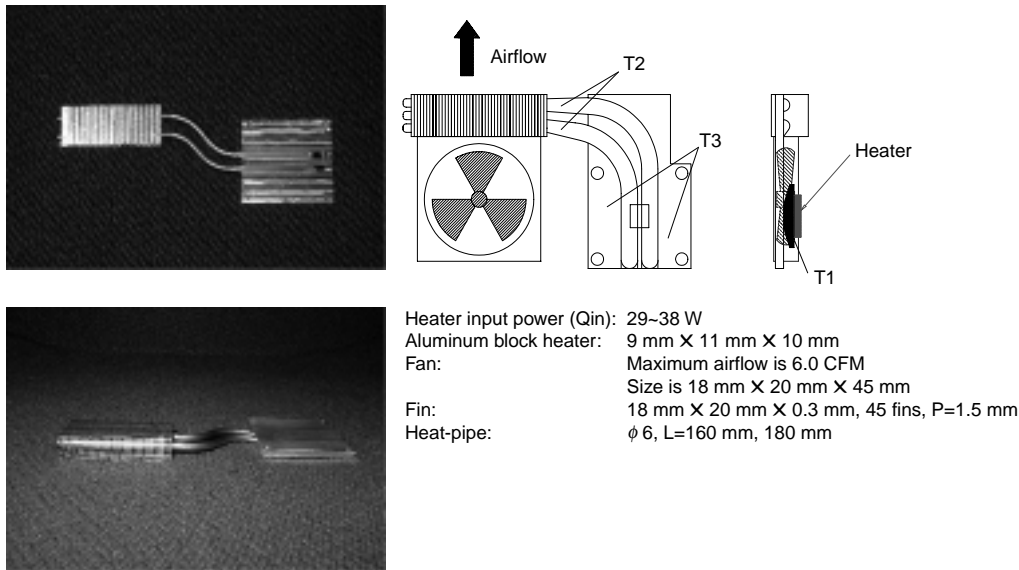


Figure 2 An example of heat sink using  $\mu$ HP.

## 2. HIGH-PERFORMANCE $\mu$ HP

Figure 2 shows an example of heat sink that employs  $\mu$ HP. One end of the  $\mu$ HP is joined to an aluminum block that is in close contact with heat generating devices such as MPU to absorb the generated heat, while the other end is installed with aluminum fins to dissipate the heat using fans, whereby efficient heat dissipation is effected thanks to the high heat-transportation characteristics of  $\mu$ HP.  $\mu$ HP per se consists of a copper pipe with a working fluid of water encapsulated therein, so that the working fluid vaporizes at the heat-absorbing end and the vaporized working fluid condenses at the heat-dissipating end. The condensed working fluid at the heat-dissipating end is returned to the vaporizing end by means of capillary force arising due to the wick structure formed on the inner surface of the copper pipe. Thus heat transportation is carried out by latent heat transfer, so that it is possible to dramatically increase the amount of heat transfer rate in comparison to ordinary heat conduction.

While wick structures of  $\mu$ HPs come in mesh, wire and sinter, most of Furukawa Electric's products employ an inner groove structure where multiple fine grooves are formed on the inner surface of a copper pipe. Advantages of the inner groove structure may be summarized as follows: the performance is relatively stabilized and the products can be manufactured at a moderate cost. The wick structure on the inner surface is an important factor that determines the performance of a  $\mu$ HP. We have developed in this study an inner groove structure of high-performance and compared it with the conventional structure. The results will be described below.

## 3. EXPERIMENTAL METHOD

Figure 3 is a schematic diagram of the measuring system. One end of a  $\mu$ HP to operate as an evaporator section

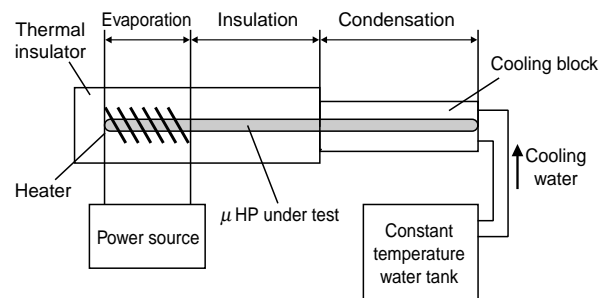


Figure 3 Schematic diagram of measuring system.

was wrapped with a heater wire at equal intervals, and voltage was applied on the heater regulating the amount of heat input. The other end to operate as a condenser section was inserted into a cooling block, and the amount of dissipation heat was regulated by the temperature of cooling water circulating in the cooling block. The intermediate portion to operate as an insulation section was thermally insulated using insulation material. Assuming sufficient insulation, the amount of heat on the evaporator section was defined as a heat transfer rate.

## 4. EXPERIMENTAL RESULTS

### 4.1 Thermal Characteristics of $\phi$ 4-mm High-Performance $\mu$ HP

#### 4.1.1 Outer Surface Temperature Distribution

Figure 4 shows a typical temperature distribution on the outer surface of a  $\phi$ 4-mm high-performance  $\mu$ HP in operation.

When the heat transfer rate is comparatively low --10 W or smaller, the outer surface temperature distribution along the entire length is almost even at the operation temperature. As the heat transfer rate increases the outer surface temperature at the evaporator section gradually

raises, while the outer surface temperature at the condenser section declines. Then the outer surface temperature at the end of the evaporator section begins to rise when a certain level of heat transfer rate is arrived at. This is caused by "dryout" of the inner surface that manifests itself as the amount of heat input reaches the maximum heat transfer rate. On the contrary, the temperature declines at the end of the condenser section. This is thought to be due to an accumulation of excessive working fluid on the condenser section end preventing heat transfer.

#### 4.1.2 Thermal Resistance

Thermal resistance is one of the important characteristics of  $\mu$ HPs. Thermal resistance can be calculated as follows:

$$\text{Thermal resistance } (^{\circ}\text{C}/\text{W}) = \frac{\text{(Average outer surface temperature of evaporation section - Average outer surface temperature of condenser section)} / \text{Heat transfer rate}}$$

Thus, when a certain temperature difference exists between the outer surface temperatures of the evaporator and condenser sections of a  $\mu$ HP, the amount of heat transferable is determined by the thermal resistance of that  $\mu$ HP.

Figure 5 shows the thermal resistance of a  $\phi 4$ -mm high-performance  $\mu$ HP in comparison to that of a conventional  $\mu$ HP.

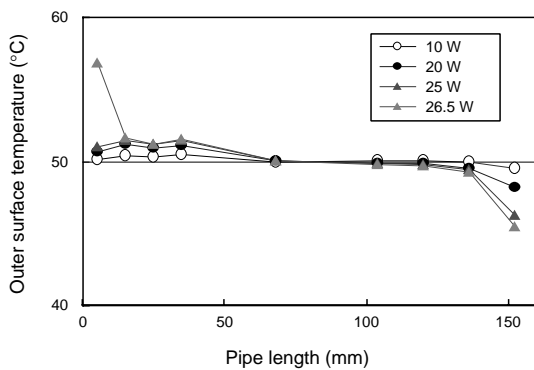


Figure 4 Outer surface temperature distribution of  $\phi 4$   $\mu$ HP.

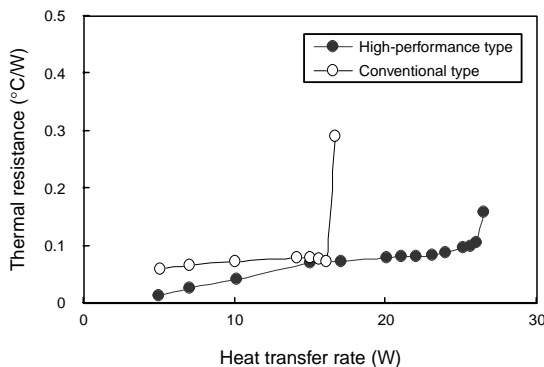


Figure 5 Thermal resistance of  $\phi 4$  high-performance  $\mu$ HP in comparison to conventional  $\mu$ HP.

It is said that a  $\mu$ HP with a wick structure of inner groove has, because the wick is formed directly on its inner surface, a lower thermal resistance in comparison to other types such as the mesh or wire types. Accordingly, a conventional  $\mu$ HP of inner groove type is seen to have a low thermal resistance of  $0.1^{\circ}\text{C}/\text{W}$  or less when the heat transfer rate is below  $10 \text{ W}$ , but the high-performance  $\mu$ HP has a thermal resistance that is improved further. What is more, whereas the conventional type reaches the maximum heat transfer rate at a little over  $15 \text{ W}$  showing a rapid increase in thermal resistance thereafter, the thermal resistance of the high-performance type remains low until the maximum heat transfer rate is reached at  $25 \text{ W}$  or over.

#### 4.1.3 Maximum Heat Transfer Rate

As described above,  $\mu$ HP-based heat sinks deteriorate in thermal resistance when a heat load exceeding the maximum heat transfer rate is applied, rising drastically in the temperature at the heat-absorbing end. Improving the maximum heat transfer rate is therefore one of the important issues of  $\mu$ HPs.

Figure 6 shows the maximum heat transfer rate of a  $\phi 4$ -mm high-performance  $\mu$ HP in comparison to that of a conventional  $\mu$ HP.

It is seen that the high-performance type dramatically outperforms the conventional type by 160~200 % at the operation temperatures of  $40\sim 70^{\circ}\text{C}$  where  $\mu$ HPs are generally used, demonstrating that the improvement in the inner groove shape of the high-performance type has been very effective in enhancing the maximum heat transfer rate.

#### 4.1.4 Effects of Inclination

It is known that, since the working fluid in a  $\mu$ HP is influenced by gravity, the maximum heat transfer rate is maximized when the  $\mu$ HP is installed with its evaporator section down, i.e., bottom-heat mode. To the contrary, when the evaporator section comes upside, i.e., top-heat mode, the working fluid condensed in the condenser section has to be transferred to the evaporator section defying gravity, making performance degradation in the  $\mu$ HP hardly avoid-

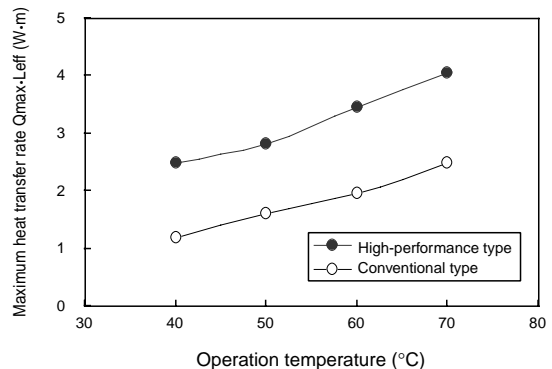
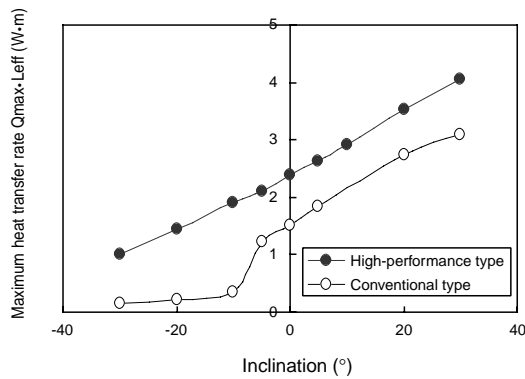
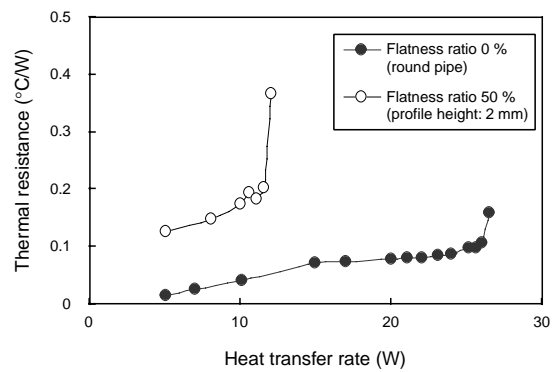


Figure 6 Maximum heat transfer rate of  $\phi 4$  high-performance  $\mu$ HP in comparison to conventional  $\mu$ HP.



**Figure 7** Maximum heat transfer rate of  $\phi 4$  high-performance and conventional  $\mu$ HPs vs. inclination.



**Figure 8** Thermal resistance of flattened  $\phi 4$  high-performance  $\mu$ HPs.

able because the transfer of the working fluid depends entirely on the capillary force of the wick.

At this time, experiments were carried out within an inclination range of  $\pm 30^\circ$  with respect to horizontal installation of  $\mu$ HP, assuming the bottom-heat mode configuration to be positive inclination while the top-heat mode negative.

Figure 7 shows the influence of inclination on the maximum heat transfer rate.

Both the high-performance and conventional types show improved performance in the bottom-heat mode. In the top-heat mode, while the conventional type suffers a sharp decline in the maximum heat transfer rate below an inclination of  $-5^\circ$ , the high-performance type shows a modest decline. Thus the difference in the maximum heat transfer rates of the conventional and high-performance products is maximized at between  $-10^\circ$  to  $-20^\circ$ . The fact that the high-performance type has been improved most significantly in the top-heat mode demonstrates that the enhancement in capillary force resulting from the improved inner groove shape has been remarkably effective in enhancing the maximum heat transfer rate.

#### 4.1.5 Characteristics of Flattened $\mu$ HP

As notebook PCs are required to be downsized,  $\mu$ HPs are frequently used with their partial or entire length flattened. Hence we have measured the thermal characteristics of  $\phi 4$ -mm  $\mu$ HPs of high-performance type when they are flattened. Flatness ratio was calculated as follows:

$$\text{Flatness ratio (\%)} = \frac{(\text{Outer diameter of pipe before flattening} - \text{Profile height of pipe after flattening})}{\text{Outer diameter of pipe before flattening}} \times 100$$

Figures 8 and 9 show the thermal resistance and maximum heat transfer rate of flattened  $\mu$ HPs, respectively.

The thermal resistance increases as the  $\mu$ HP becomes more flat, thereby tending to impede the thermal performance. The maximum heat transfer rate also tends to deteriorate as the flatness ratio raises. Even though the high-performance type has higher maximum heat transfer rate than the conventional type when flattened, it has a

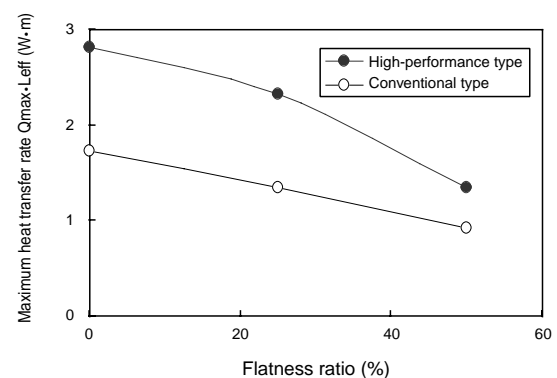


**Figure 9** Maximum heat transfer rate vs. flatness ratio of  $\phi 4$   $\mu$ HPs.

larger rate of performance degradation with respect to flatness ratio.

#### 4.2 Effects of Pipe Diameter

As described above, it was seen that  $\phi 4$ -mm  $\mu$ HPs of high-performance type have dramatically improved in thermal characteristics including maximum heat transfer rate. We then proceeded to fabricate  $\phi 5$ -mm and  $\phi 6$ -mm  $\mu$ HPs of high-performance type with improved inner groove structure to investigate their thermal characteristics.

Figure 10 shows the maximum heat transfer rates of  $\phi 4$ -mm through  $\phi 6$ -mm  $\mu$ HPs of high-performance type.

The pipe diameter is seen to have substantial effects such that the larger the pipe diameter, the greater the maximum heat transfer rate improves. In particular, the high-performance type exhibits greater effects of improvements in the maximum heat transfer rate.

Figure 11 shows the maximum heat transfer rates of  $\phi 4$ -mm through  $\phi 6$ -mm  $\mu$ HPs of high-performance type that are flattened to a profile height of 2 mm. As without flattening, the maximum heat transfer rate dramatically improved as the pipe diameter increased, but when flattened, the effects of the pipe diameter prior to flattening tends to diminish. This is because the larger the pipe diameter the greater the flatness ratio becomes when the pipe is flattened to a profile height of 2 mm, resulting in a greater decline of maximum heat transfer rate.

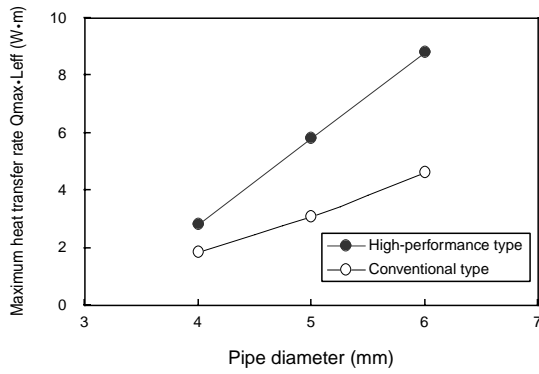


**Figure 10** Maximum heat transfer rate of large-sized  $\mu$ HPs.

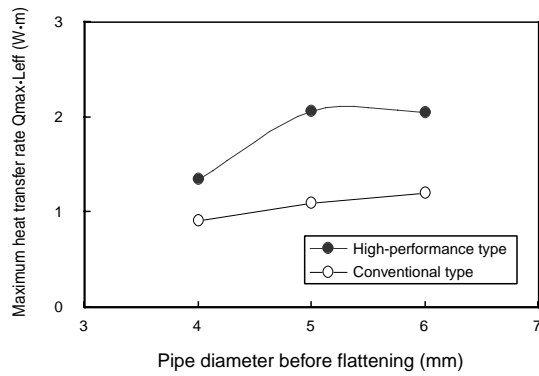


**Figure 11** Maximum heat transfer rate of flattened  $\mu$ HPs with a profile height of 2 mm.

## 5. IN CONCLUSION

Furukawa Electric has been developing, beginning since 1995, heat sinks that incorporate  $\mu$ HPs to cope with the ever increasing heat brought about by greater electronic equipment speeds and higher performance. This paper describes improvements in the thermal characteristics of  $\mu$ HPs achieved by optimizing the inner groove structure. Thus with respect to  $\phi$ 4-mm through  $\phi$ 6-mm  $\mu$ HPs of high-performance type, we have been successful in drastically improving the thermal characteristics including maximum heat transfer rate in comparison to conventional types. We hope these improvements can be effectively applied in heat sinks so as to deal with the growing heat generation of electronic equipment expected in future.

## REFERENCES

- 1) Oomi and Fukumoto: Furukawa Review No.21, p.69 (2002)